JDI Journal of Diabetes Investigation Open access
Official Journal of the Asian Association for the Study of Diabetes
ORIGINAL ARTICLE

Induction of proximal tubular proliferation and lengthening in response to sodium glucose linked cotransporter-2 inhibition in experimental rats

Ellen Wu[1,2], Sarah Macklin[1,2], Yanling Zhang[1,2], Kerri Thai[1,2], Linda Nghiem[1,2], Caterina Di Ciano-Oliveira[1,2], Nuno Coelho[1,2], Hai Wang[1,2], Suzanne L. Advani[1,2], Jean-François Desjardins[1,2], Darren A Yuen[1,2], Paraish Misra[2], Kim A. Connelly[1,2], Jens R. Nyengaard[3,4], Richard E. Gilbert[1,2]*

[1]Keenan Research Centre for Biomedical Science in the Li Ka Shing Knowledge Institute, St. Michael's Hospital, Toronto, Ontario, Canada, [2]Department of Medicine, University of Toronto, Toronto, Ontario, Canada, [3]Section for Stereology and Microscopy, Department of Clinical Medicine, Core Centre for Molecular Morphology, Aarhus University, Aarhus, Denmark, and [4]Department of Pathology, Aarhus University Hospital, Aarhus, Denmark

Keywords
Kidney growth, proximal kidney tubule, sodium-glucose linked cotransporter 1, 2

***Correspondence**
Richard E. Gilbert
Tel.: +1-416-867-3747
Fax: +1-416-867-3747
E-mail address:
richard.gilbert@utoronto.ca

J Diabetes Investig 2025

doi: 10.1111/jdi.70043

ABSTRACT

Aims/Introduction: While SGLT2 accounts for >90% of kidney glucose reabsorption, its pharmacological inhibition or genetic knockdown reduces glucose reabsorption by only 50%.

Materials and Methods: We postulated that the less than expected glucosuric response to SGLT2 inhibition might result from a compensatory increase in the length of the proximal tubule as seen in experimental diabetes where early tubular proliferation is followed by tubular lengthening. Taking advantage of their differing anatomical locations, stereological techniques were used to differentiate the SGLT1 expressing straight proximal tubule that lies within the outer stripe of the outer medulla (S3 segment) and that of the predominantly SGLT2 expressing early proximal convoluted tubule located within the kidney cortex (S1, S2 segments).

Results: The SGLT2 inhibitor, dapagliflozin, induced an early, transient hyperplastic response (3-fold increase of Ki67 labelling, $P < 0.0001$) in S3 proximal tubular cells followed by a 32% increase in its length ($P < 0.0001$). In contrast, the length of the SGLT2 expressing S1, S2 segments of the proximal tubule was unaffected.

Conclusions: The finding that SGLT2 inhibition leads to expansion of the S3 segment of the proximal tubule, the site of SGLT1, is suggestive of a physiological response to diminish urinary glucose loss akin to that occurring in experimental diabetes. These findings provide a cogent explanation for the less-thanthan-expected effect of this drug class on glucose reabsorption.

INTRODUCTION

Close to 100% of the roughly 180 g of glucose that enters the glomerular filtrate each day is reabsorbed. This vital physiological process takes place exclusively in the proximal tubule and is mediated by two sodium-linked cotransporters, sodium-glucose linked cotransporter-2 (SGLT2) and SGLT1. Under normal circumstances, up to 97% (160–180 g) of glucose reabsorption is mediated by SGLT2, while the remainder, a mere 3% (5 g) is undertaken by SGLT1[1]. Notably, the two transporters are localized to specific segments of the proximal tubule. SGLT2 is expressed in the early, convoluted segments of the proximal tubule (S1, S2) that reside within the kidney cortex[2]. The SGLT1-expressing straight proximal tubules (S3, *pars recta*), on the other hand, lie within the outer stripe of the outer medulla

Received 27 January 2025; revised 20 March 2025; accepted 25 March 2025

(OSOM)[3,4]. These different anatomical localizations within the kidney enable the differentiation between the S1/S2 and S3 at a light microscopic level.

While in theory, loss of SGLT2-mediated glucose transport would be expected to reduce glucose reabsorption by >90%, genetic knockdown or pharmacological inhibition only reduces it by around 50%[5]. This phenomenon applies to both the rodent and human settings where it is presumed to reflect a dramatic increase in SGLT1-mediated glucose reclamation[1] since dual SGLT1/2 knockout mice are incapable of renal glucose reabsorption[6]. The mechanism underlying this compensatory shift towards SGLT1, a high-affinity but low-capacity transporter, is, however, unknown.

We hypothesized that the increase in SGLT1-mediated glucose reclamation might reflect an increase in the size of the proximal tubule where early tubular proliferation is followed by tubular lengthening akin to that seen in experimental diabetes[7–10]. Unlike diabetes, however, where the increase in glucose load originates from the glomerular filtrate and exposes the entire proximal tubule, with SGLT2 inhibition the increase in urinary glucose originates in the S1, S2 segments so that only the S3 is maximally exposed. Accordingly, we sought to examine segmental proliferation and lengthening in the proximal tubule in response to SGLT2 inhibition, taking advantage of their differing anatomical locations and the contribution of the proximal tubule to kidney volumes in the cortex (48%) and the OSOM (54%)[11].

MATERIALS AND METHODS

Animals

Study 1

Thirty-two, 12-week-old male Sprague Dawley (SD) rats (Charles River Laboratories, Saint Constant, QC, Canada) were randomized to receive vehicle (5% 1-methyl-2-pyrrolidinone, 20% polyethylene glycol, and 20 mmoL/L sodium diphosphate) or the SGLT2 inhibitor dapagliflozin (AstraZeneca, Mississauga, ON, Canada) dosed at 0.5 mg/kg b.i.d. as previously described for rodent administration by oral gavage[12], for 6 weeks the timeline for kidney growth in the diabetes setting[10]. In 12 of the rats (six vehicle, six dapagliflozin), glomerular filtration rate (GFR) was determined using FITC-inulin just prior to termination[13].

Twenty of the animals (10 vehicle, 10 dapagliflozin) were housed in metabolic cages for 24 h to assess urine glucose (ABL825 Flex Series blood gas analyzer, Radiometer Canada) to confirm dapagliflozin's effect. To exclude extracellular fluid as a contributor to changes in kidney weight, dry kidney weight was determined by harvesting and drying the kidneys, as previously described[14].

After metabolic caging, animals were terminated for tissue collection. The right renal pedicle was clamped, following which animals underwent left-kidney perfusion with 10% formalin under 2–5% isoflurane anesthesia. The perfused (left) kidneys were used for glomerular volume measurement and kidney stereology, and the non-perfused (right) kidneys were collected for kidney weights (wet and dry).

Study 2

A study of 48 rats was undertaken to determine whether hyperplasia contributed to kidney growth. Kidneys were examined at 1, 2, 3, and 7 days ($n = 6$ vehicle, $n = 6$ dapagliflozin at each time point), replicating the time course for radiolabeled thymidine incorporation in diabetic and uninephrectomized rats[7]. Animals were terminated and their kidneys harvested. The left kidney was fixed in formalin for subsequent in situ hybridization and immunohistochemistry, and the right kidney was frozen in optimal cutting temperature (OCT) compound (Tissue-Tek; Sakura Finetek, Torrance, CA, USA) for subsequent immunofluorescence, as previously described[15].

Tissue collection

Animals were anesthetized with 2–5% isoflurane, and a 4–5 cm incision was made in the anterior abdominal wall to access the kidneys and major vessels. The right renal artery and vein were clamped, followed by removal of the right kidney for weighing before being snap frozen in liquid N_2 prior to storage at −80°C. Perfusion fixation of the left kidney was undertaken, as previously reported[16]. Perfused left kidneys were then cut into 3 mm isotropic, uniform, and random (IUR) slabs using the two-step orientator method to allow for a design-unbiased tubule length estimation, as previously described[17,18].

Kidney morphology

Kidney volume, glomerular volume, and tubular length were all calculated on perfusion fixed kidneys. As previously reported[18], kidney volume was estimated using the equation:

$$V(\text{kid}) = W(\text{kid})/\rho,$$

where W (kid) is the perfused kidney weight, and ρ (1.04 g/cm^3) is the weight-to-volume ratio of kidney tissue.

Glomerular volume

Glomerular volume was estimated using the model-based method of Weibel and Gomez, as previously described[19]. In brief, 30–50 glomerular profiles were randomly sampled from the H&E-stained slides and scanned with a Zeiss Axioscan.Z1 slide scanner microscope system prior to image analysis (HALO image analysis platform, Indica Labs, Albuquerque, NM, USA). The glomerular cross-sectional area (GA) was then used to calculate the glomerular volume using the following equation:

$$\text{GV} = \frac{\beta}{k}(\text{GA})^{3/2},$$

where β (1.38) pertains to spheres, and k (1.10) is the distribution coefficient.

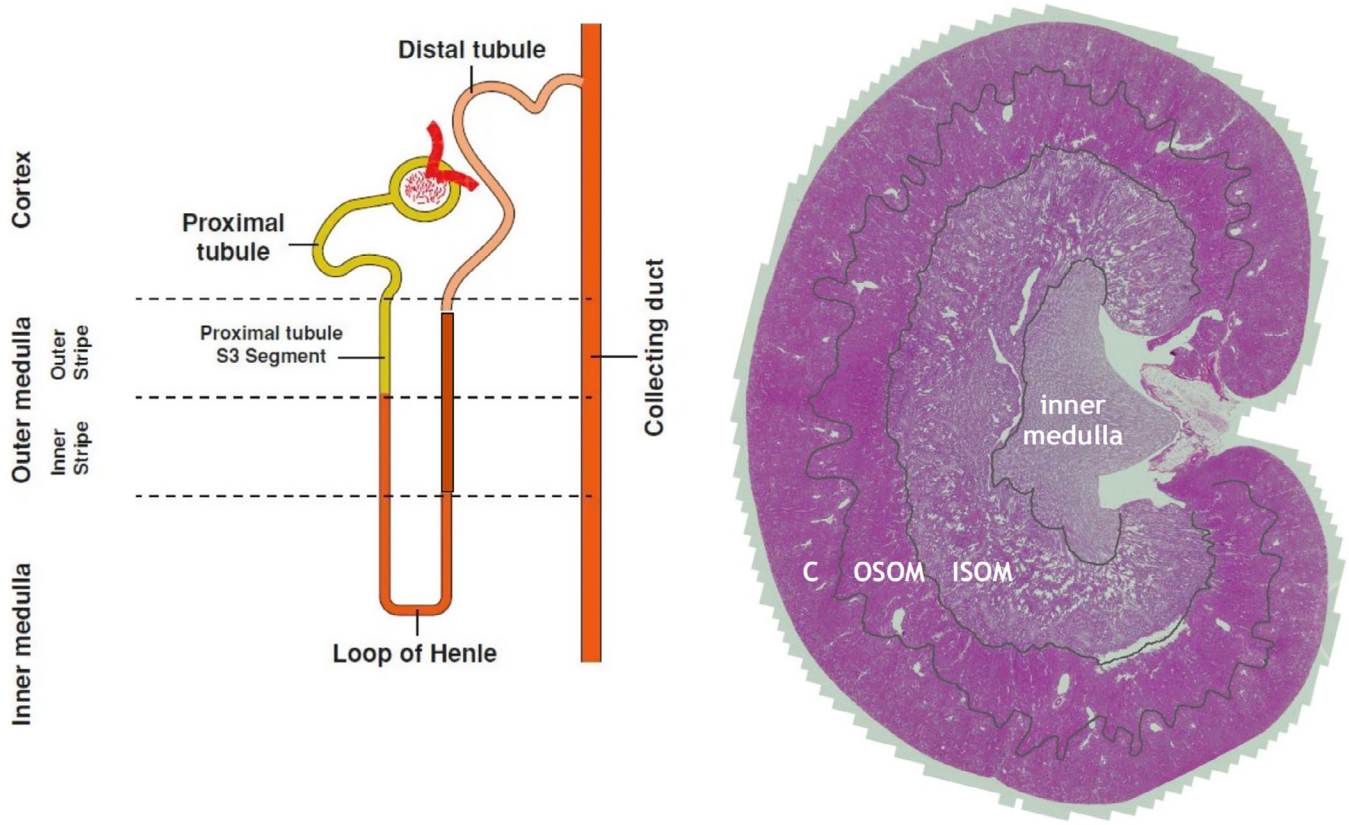

Figure 1 | Diagram showing location of the proximal convoluted tubule (S1, S2) within the kidney cortex and the straight or *pars recta* portion (S3) lying within the outer stripe of the outer medulla (left) https://aneskey.com/renal-physiology-and-its-systemic-impact (accessed January 10, 2025). PAS stained, sagitally sliced rat kidney with line tracings to show the demarcation of anatomical zones of the kidney as cortex (C), outer stripe of outer medulla (OSOM), inner stripe of outer medulla (ISOM) and inner medulla.

Kidney volumes

Kidney volumes were calculated using the equation:

$$V(\text{kid}) = W(\text{kid})/\rho,$$

where V (kid) is the estimated kidney volume, W (kid) is the perfused kidney weight, and ρ (1.04 g/cm^3) is the weight-to-volume ratio of kidney tissue. The relative proportions of cortex and medullary sizes were measured via the unbiased point counting method from approximately four isotropic, uniform, random sections per kidney, as described below for tubular length.

The estimated cortical (cor) and medullary (med) sizes were then calculated using the following equations:

$$V(\text{cor}) = V(\text{kid}) \times V_v(\text{cor/kid}) \text{ and}$$
$$V(\text{med}) = V(\text{kid}) \times V_v(\text{med/kid}),$$

where V (cor) is the estimated cortical volume, V (med) is the estimated medullary volume, V_v (cor/kid) is the relative proportion of cortex over total kidney size, and V_v (med/kid) is the relative proportion of medulla over total kidney size.

Tubule length

Proximal tubules were identified by their prominent brush border and cuboidal appearance in periodic acid-Schiff (PAS)-stained sections[8], separately analyzing the lengths of the early proximal tubule (S1, S2) that lie within the cortex and the late proximal tubule (S3) located in the OSOM (Figure 1).

Tubule length was calculated as previously described[18]. In brief, PAS-stained, perfused kidney samples were scanned at 20× bright-field using the Zeiss Axioscan.Z1 slide scanner microscope system. From the scanned images, 30–50 equal-sized fields of view were selected using systematic sampling and analyzed using the two-dimensional unbiased counting frame[18]. Using a computer-based image processing software with a built-in cell counter plugin[20, 21], two unbiased counting grids were superimposed on each image, from which cells of the proximal tubules and those of the more distal nephron were separately counted (Figure 2). The total number of

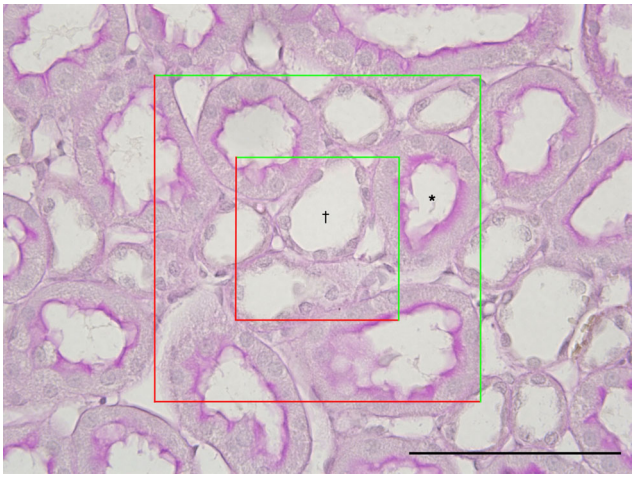

Figure 2 | Proximal tubule and distal nephron profiles were counted using two unbiased counting frames (23,716 μm^2 [inner square] and 108,900 μm^2 [+outer square] for PT and DN, respectively). Proximal tubules were recognized by their cuboidal appearance and PAS positive brush border (*) in contrast to the thin, PAS negative cells of the distal nephron (†). Structures were counted if they touched the inclusion (green) lines and were excluded if they touched the exclusion (red) lines. PAS stain. Final magnification 30×. Scale bar: 100 μm.

sampled profiles for each structure (Q(tub)) was then used to calculate the respective length densities of proximal and distal nephron, using the following equation:

$$L_v(\text{tub/cor}) = \frac{2 \bullet \Sigma Q(\text{tub})}{a\ (\text{frame}) \bullet \Sigma P(\text{cor})},$$

where (frame) is the area associated with a counting frame (23,716 and 108,900 μm^2 for proximal and distal nephron, respectively); P (cor) is the total number of points hitting the renal cortex.

Since the tubule length densities were estimated relative to the cortex, the relative volume of cortex in the kidney was also required to estimate the tubule lengths. Test points were superimposed on the images, and the number of points hitting the cortex and medulla was counted using the ZEN (blue edition) software. The relative cortex volume was calculated as follows:

Table 1 | Body weight, urinary glucose excretion, glomerular volume and filtration rate in control and dapagliflozin-treated rats

	Vehicle	Dapagliflozin
Body weight (g)	566 ± 48	530 ± 38
Urinary glucose (mmol/day)	0.01 ± 0.00	28.5 ± 4.9*
GFR (μL/min/g)	5.2 ± 0.8	5.3 ± 1.1
Glomerular volume (μm^3)	1.2 ± 0.2	1.3 ± 0.1

Data as mean ± SD. *$P < 0.001$.

$$V_v(\text{cor/kid}) = \frac{P(\text{cor})}{P(\text{kid})},$$

where P (cor) is the number of points hitting the cortex, and P (kid) is the number of points hitting the kidney.

Finally, proximal tubule length was calculated using the equation:

$$L_T(\text{tub}) = L_v(\text{tub/cor}) \bullet V_v\ (\text{cor/kid}) \bullet V(\text{kid}),$$

where L_v (tub/cor) is the relative tubule length density in the cortex, V_v (cor/kid) is the relative cortex volume, and V (kid) is the kidney volume estimated by kidney weight. Both L_v (tub/cor) and V_v (cor/kid) are calculated after tissue processing-induced shrinkage.

Cell proliferation

Perfusion-fixed left kidneys were sectioned and immunostained with anti-Ki-67 antibody to assess renal cell proliferation, as previously described[22] using Ki-67 (mouse monoclonal anti-rat Ki-67 antigen, clone MIB-5, DakoCytomation, Glostrup, Denmark) in 15 randomly selected fields of view (Halo Image Analysis Platform, Indica Labs).

In situ hybridization

To confirm that SGLT1 expression was confined to cells with PAS +ve brush borders lying within the OSOM, site-specific expression of SGLT1 was determined by in situ hybridization. This was undertaken using RNAscope (Advanced Cell Diagnostics, Hayward, CA, USA) according to the manufacturer's instructions with custom software, as previously described[23], using a probeset specific for rat SGLT1. Hybridization signal was detected using Fast Red, with hybridized RNA identifiable as red puncta on light microscopy. To determine whether SGLT1-expressing cells were undergoing proliferation, 5 μm serial sections were obtained and subjected to in situ hybridization for SGLT1, with the following section immunostained for Ki-67, as described above.

Immunofluorescence

Kidney cryosections (16 μm thickness) were fixed with cold 4% paraformaldehyde for 15 min and rinsed with PBS, followed by 10 min immersion in permeabilization buffer (0.1% Triton X-100 in 1xPBS). Sections were subsequently rinsed with PBS, blocked with 5% BSA for 1 h 30 min, and stained with primary antibodies for SGLT1 (PA5-37937, Invitrogen, Whitby, ON, Canada) and nephron segment specific markers NKCC2 (ab191315, Abcam, Cambridge, UK; thick ascending loop of Henle), NCC (AB3553, Millipore, Burlington, MA, USA; distal tubule), AQP2 (PA5-78808, Invitrogen; sc-515770, Santa Cruz Biotechnology, Dallas, TX, USA; collecting duct) at 4°C in a humidified chamber. Sections were allowed to warm up at room temperature for 1 h before rinsing with PBS for 6 × 10 min, followed by incubation with secondary antibodies, Alexa Fluor 488 donkey anti-goat

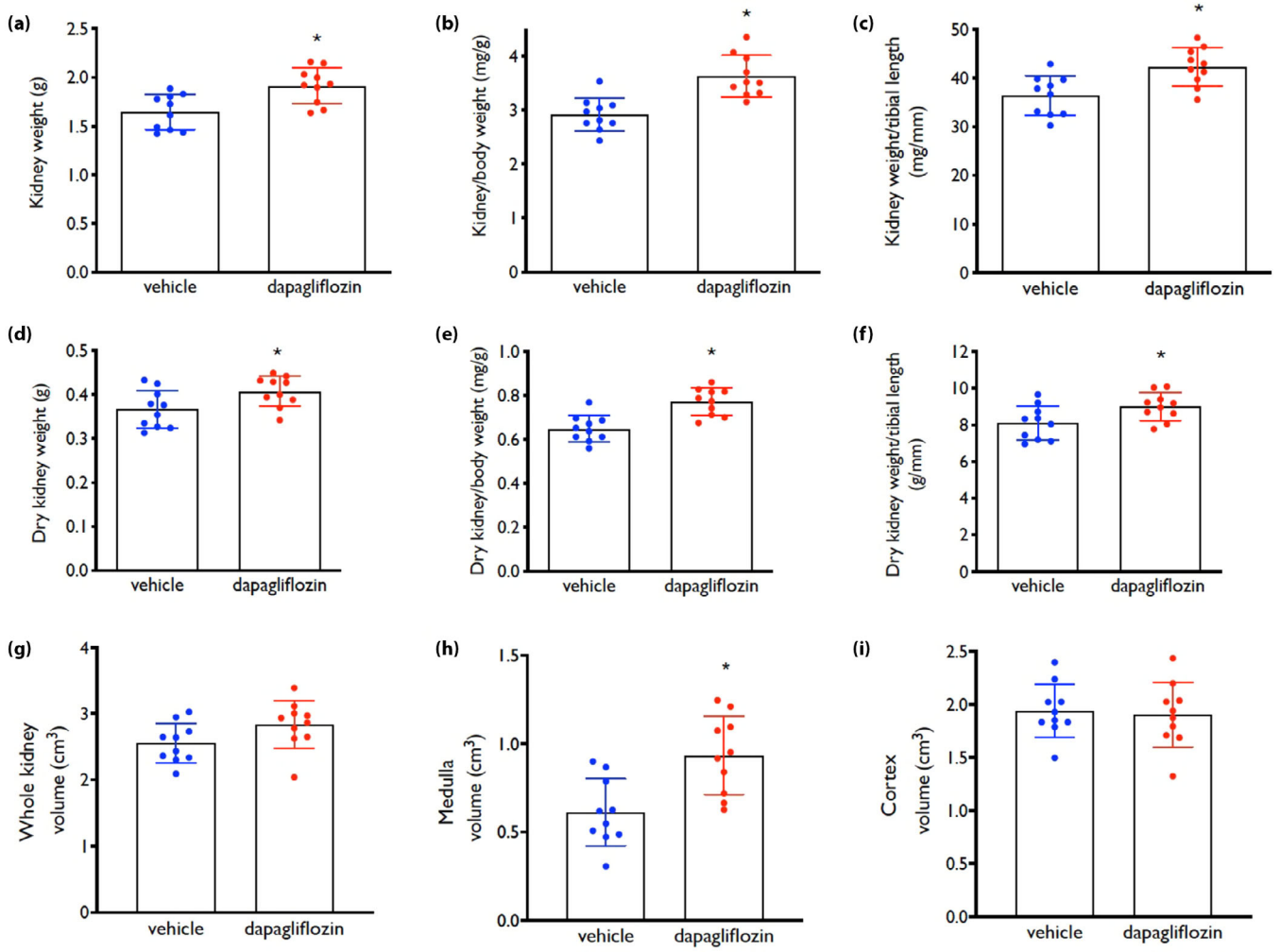

Figure 3 | Kidney weight (upper panel, a–c) and dry kidney weight (middle panel, d–f) and kidney volumes (g–i) in vehicle (●) and dapagliflozin-treated (●) rats. Kidney weights were expressed relative to body weight (b, e) and tibial length (c, f). Kidney volumes were assessed in whole kidney (g), medulla (h) and cortex (i). Data are expressed as mean ± SD. Each dot represents an individual rat. *$P < 0.01$.

IgG, and Alexa Fluor 647 donkey anti-rabbit IgG (ThermoFisher Scientific, Whitby, Ontario, Canada), and Alexa Fluor 488 donkey anti-mouse IgG for 2 h at room temperature. After rinsing with PBS for 6 × 10 min, slides were count-stained with nucleic acid dye, Hoechst 33342 (Thermo Scientific, Rockford, IL, USA) and mounted with anti-fade fluorescence mounting medium (Abcam). Fluorescent images were taken on Zeiss LSM700 with a 20× objective.

Glomerular filtration rate

Before termination, rats underwent glomerular filtration rate (GFR) measurement using a modified fluorescein isothiocyanate (FITC)-inulin plasma clearance assay, as previously reported[24]. Briefly, rats were injected in the tail vein with 3.74 mL/g body weight FITC-inulin. Tail vein blood was sampled at various time points after FITC-inulin injection. Sample fluorescence was detected using a Fluoroscan Ascent FL machine (Thermo Scientific) with settings of 485 nm excitation and 538 nm emission. GFR was calculated using the following two-phase, exponential decay curve using nonlinear regression statistics, as also previously described[24], where $GFR = I/(A/ + B/)$, where I is the amount of FITC-inulin injected, A and B are the y-intercept values for the two decay rates, and are the decay constants for the distribution and elimination phases.

Statistics

Data are expressed as mean ± SD unless otherwise specified. Statistical significance was determined using 2-way ANOVA with Tukey's multiple comparison post hoc test and unpaired Student's t-test on GraphPad Prism 8 (GraphPad Software, San Diego, CA, USA). A P value of less than 0.05 was considered statistically significant.

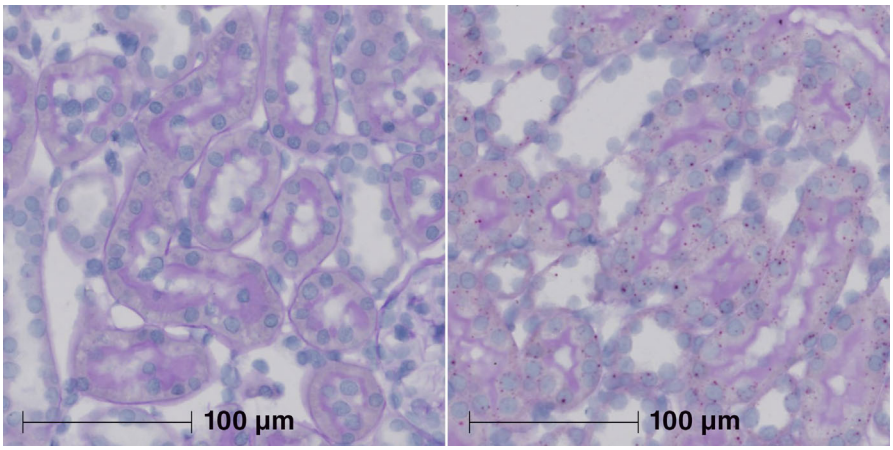

Figure 4 | Representative photomicrograph of *in situ* hybridization for SGLT1 mRNA in PAS-stained kidney sections of kidney cortex (left) and OSOM (right). Proximal tubules are identified by their PAS +ve luminal brush border staining (thick juxtalumenal magenta band). Punctae of SGLT1 mRNA are evident in proximal tubules from the OSOM but not the cortex. Final magnification 20×.

RESULTS

Animal characteristics

After 6 weeks, dapagliflozin led to glucosuria in all animals so treated and was also associated with a numerical reduction in body weight that did not reach statistical significance (Table 1).

Kidney size

Kidney weight and kidney weight indexed to either body weight or tibial length were increased in rats that had received dapagliflozin over the preceding 6 weeks (Figure 3). To account for the effect of intra- or extracellular fluid retention on kidney weight, dry kidney weights were also analyzed and expressed relative to body weight and tibial length, showing changes similar to the freshly harvested organs (Figure 3).

A numerical but not statistically significant 11% increase in whole kidney volume ($P = 0.07$) was evident in rats that had received dapagliflozin compared with those administered vehicle for the preceding 6 weeks (Figure 3). Medullary volume, however, changed substantially more with an approximate 50% increase in volume among rats assigned to receive dapagliflozin ($P < 0.01$) consistent with the expansion of the proximal tubule in this region. By contrast, no between-group differences in cortical volumes were seen.

In situ hybridization and immunolabeling

In situ hybridization confirmed that SGLT1 expression was confined to the S3 segment of the proximal tubule as identified by the presence of abundant SGLT1 mRNA puncta within cuboidal cells with PAS +ve luminal brush borders located in the outer stripe of the outer medulla (OSOM, Figure 4). By contrast, SGLT1 mRNA puncta were not seen in brush border −ve cells within the OSOM, nor in brush border +ve cells in the cortex of PAS-stained sections. Double-labeled immunofluorescence (Figure 5) confirmed the absence of SGLT1 expression in the thick ascending loop of Henle (NKCC2), distal tubule (NCC) or collecting duct (AQP2).

Proliferation

Cell proliferation, identified by the extent of Ki67 labeling, was different between vehicle and dapagliflozin-treated rats ($P < 0.0001$). Cell proliferation peaked at Day 2 with a three-fold increase in Ki67 immunolabeling in dapagliflozin-treated rats before rapidly diminishing so that it was no longer evident by Day 7 (Figure 6). The increase in Ki-67 immunolabeling on Day 2 was confined to the S3 segment of proximal tubules. Serial sections employing in situ hybridization for SGLT1 mRNA and Ki67 immunolabeling confirmed that these brush border PAS +ve cells expressed both SGLT1 and Ki67 (Figure 7). No increase in labeling was observed in glomeruli, in the kidney cortex, or in other cell types within the OSOM. Vehicle-treated rats showed no change in cell proliferation throughout the course of the study in either tubular cells or in glomeruli.

Proximal and distal tubule length

Using gold standard stereological methodology to determine proximal tubular length, dapagliflozin-treated rats displayed a near-doubling in length of the S3 segment when compared with animals that had received vehicle at 6 weeks ($P < 0.01$, Figure 8). The length of the SGLT2 expressing S1/S2 segments of the proximal tubule located in the kidney cortex was, in contrast, unaffected by the administration of dapagliflozin.

Glomerular changes

After 6 weeks, GFR was similar in vehicle and dapagliflozin-treated rats (Table 1). Similarly, no difference in glomerular volume between dapagliflozin-and vehicle-treated animals was noted either.

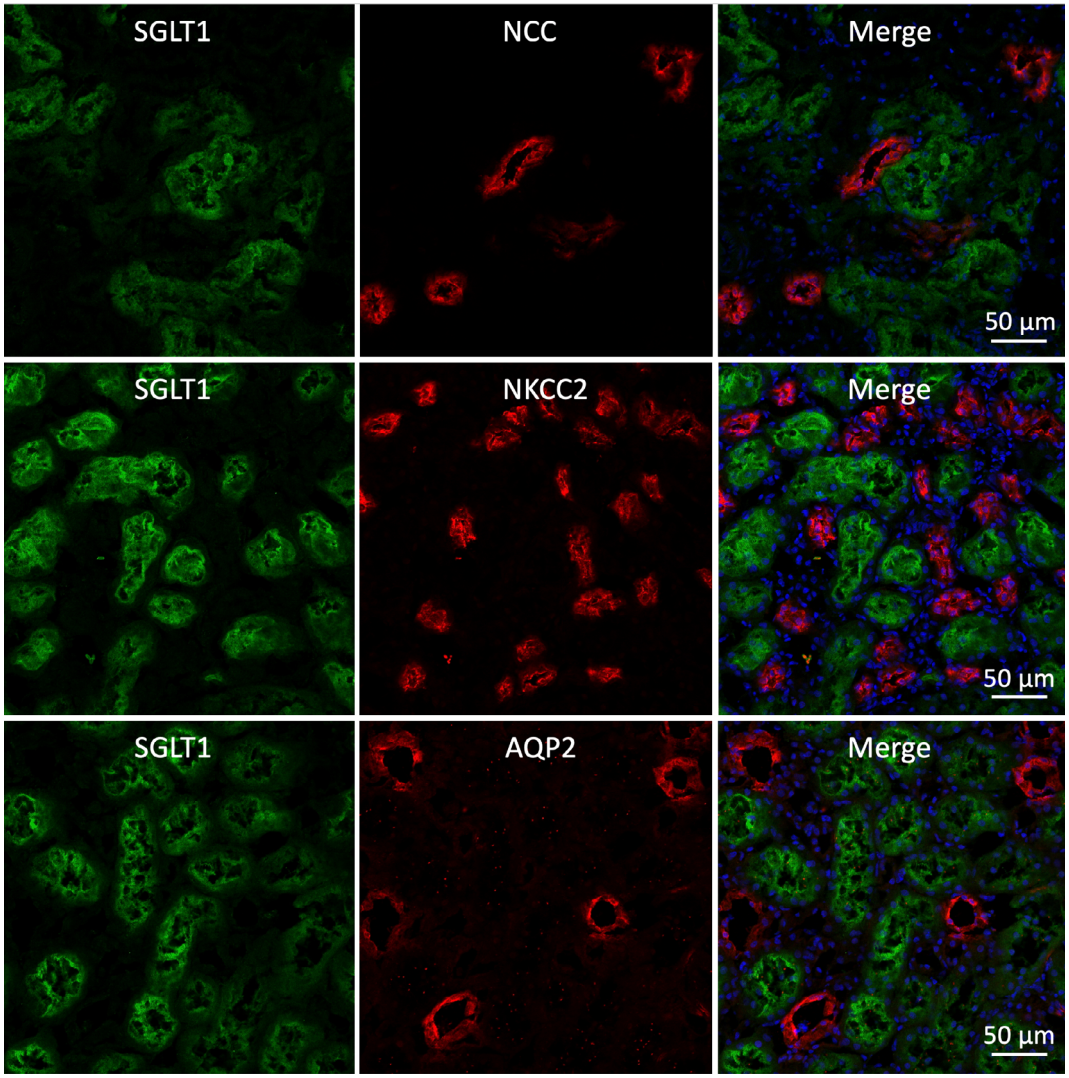

Figure 5 | Representative photomicrographs of kidney sections examined by double-labeled immunofluorescence for SGLT1 and nephron-specific markers showing the absence of colocalization in the thick ascending loop of Henle (NKCC2), distal tubule (NCC), and collecting duct (AQP2). Final magnification 20×.

DISCUSSION

Mammalian life evolved in a world where calories were scarce. As such, mitigating insensible energy-providing nutrient loss in the feces or urine was fundamental to survival. When this physiology is disturbed, as for instance in the glucosuria that develops in diabetes, the proximal tubule lengthens, ostensibly to increase the kidney's capacity to reabsorb glucose and reduce energy loss[10]. The observation that the glucosuric effect, of SGLT2 inhibitors is substantially less than anticipated from this transporter's contribution to renal glucose reabsorption is also consistent with this notion[1]. With only two transporters, SGLT1 and SGLT2, that are together responsible for reabsorbing the entirety of glucose appearing in the glomerular filtrate[6], the present study goes some way to explaining the underlying mechanism, showing that selective inhibition of SGLT2 leads to lengthening of the unaffected SGLT1-expressing S3 segment of the proximal tubule. By contrast, lengthening of the SGLT2-containing cortical segment of the proximal tubule would not affect a reduction in glucosuria in the presence of continued pharmacological inhibition of the transporter and, accordingly, does not increase.

Of the two transporters, the vast majority of glucose reabsorption is mediated by the low affinity/high capacity SGLT2, while the high affinity/low capacity SGLT1 is relegated to mopping up the small remainder[25]. However, rather than inhibiting 90–97% of glucose reabsorption, pharmacological inhibition of SGLT2 leads to only 50% of the predicted inhibition[1]. To date, a number of hypotheses have been put forward to account for

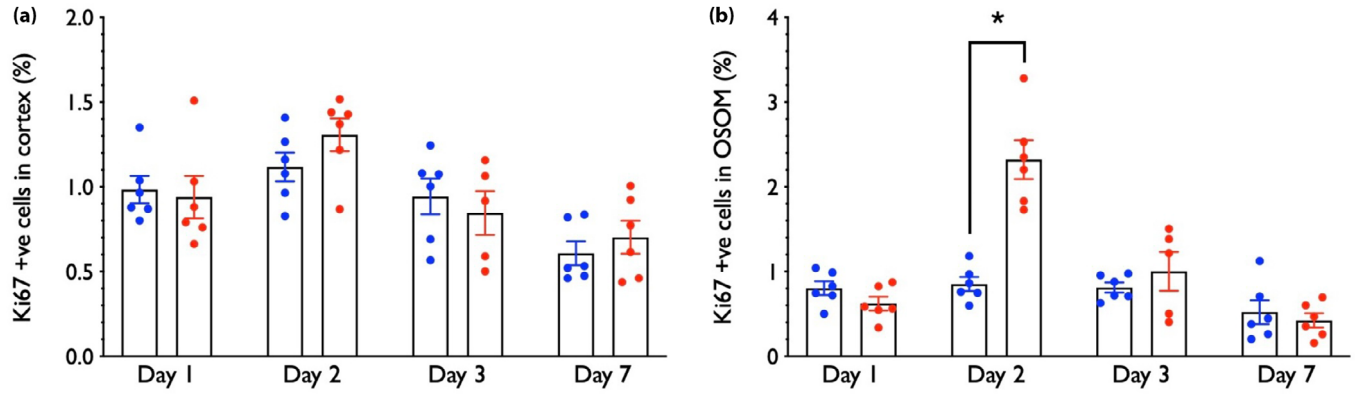

Figure 6 | Time course of Ki67 labelling in kidneys of vehicle (●) and dapagliflozin-treated (●) rats in kidney cortex (a) and outer stripe of outer medulla (OSOM, b) after 2 days of vehicle (c) or dapagliflozin administration. Data are expressed as mean ± SD. Each dot represents an individual rat. *$P < 0.001$.

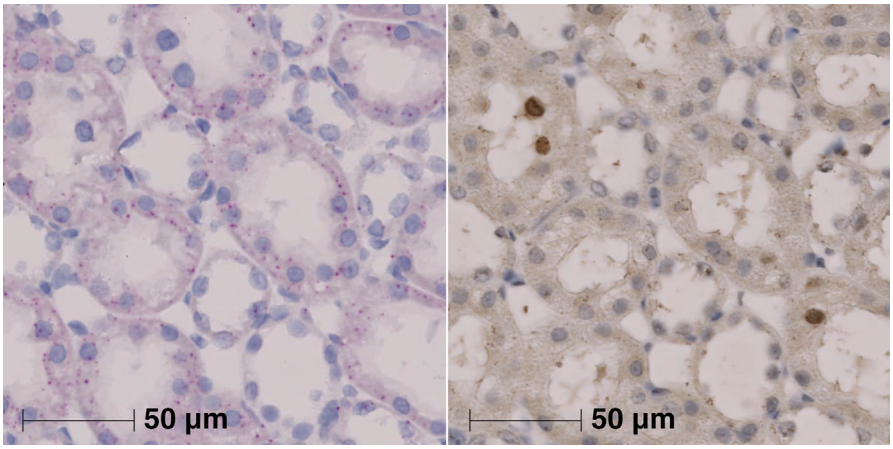

Figure 7 | Illustrative photomicrographs of serial sections showing *in situ* hybridization for SGLT1 mRNA (left) and Ki67 nuclear immunolabeling (right) in the OSOM 2 days after dapagliflozin administration indicating SGLT1 +ve cells undergoing proliferation. Final magnification 20×.

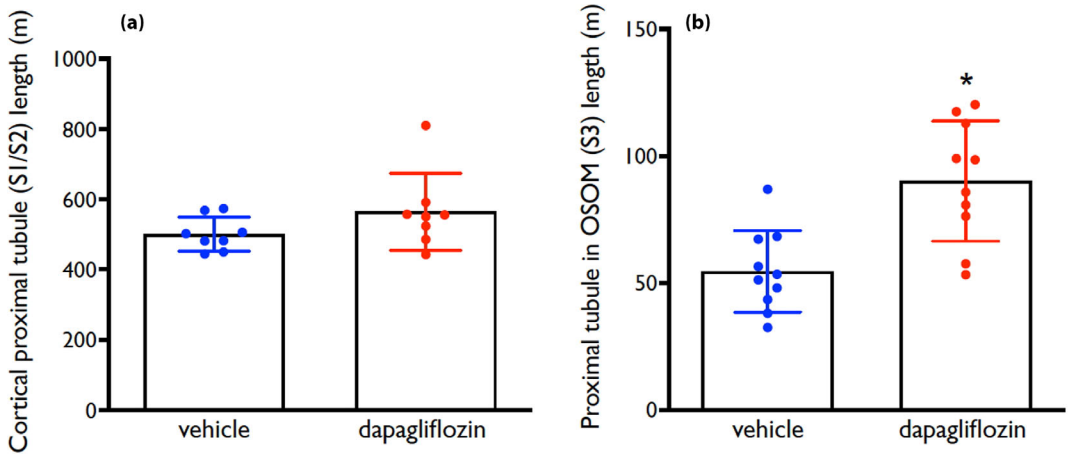

Figure 8 | Length of the proximal convoluted tubule (S1/S2) in the cortex (a) and its straight segment (S3) in the outer stripe of outer medulla (b) after 2 weeks of vehicle (●) or dapagliflozin (●) administration as measured on PAS-stained section using the two-dimensional unbiased counting method. Data are expressed as mean ± SD. Each dot represents an individual rat. *$P \leq 0.001$.

the less than predicted effect of SGLT2 inhibitors on glucose reabsorption, many of which relate to the pharmacodynamic properties of the drugs[5]. However, similar effects on glucose reabsorption are observed when SGLT2 is genetically deleted rather than inhibited pharmacologically[26]. And while the upregulation of SGLT1 had been proposed as a possible compensatory mechanism to counteract excess urinary glucose loss, its expression in the kidney is not increased with SGLT2 knockdown[26]. The current study suggests, rather, that an increase in the length of the SGLT1-containing S3 component of the proximal tubule accounts for the diminutive glucosuric response to SGLT2 inhibition.

Increase in the length of the proximal tubule is a well-described phenomenon following the onset of streptozotocin-induced diabetes[10]. In that setting, tubular length increases rapidly following induction of streptozotocin-induced diabetes[10]. As in the present study, proximal tubular cell proliferation in diabetes is also readily detected in diabetes with a notable peak 2 days after the onset of glucosuria, followed by a rapid return to basal conditions[7]. Unlike in the present study, however, proximal tubular lengthening was accompanied by substantial glomerular enlargement and an increase in GFR[10]. Further unlike the current study, proximal tubular measurements in diabetes have been confined to the cortex and did not include the S3 component of the proximal tubule that lies within the OSOM.

The finding that a member of a nephroprotective drug class induces an increase in kidney size may also seem at first glance somewhat paradoxical. Several large-scale clinical trials have consistently shown that SGLT2 inhibitors reduce the rate of kidney function loss, yet nephromegaly is often linked to an adverse prognosis in diabetic kidney disease[27, 28]. This may, however, be more guilt by association than causation since nephromegaly is frequently accompanied by glomerular hyperfiltration, itself an adverse prognostic sign[29, 30]. The two phenomena, however, are not inextricably linked[22,31,32] as also shown in the current study where nephromegaly occurs without a commensurate increase in GFR.

The strengths of this study center on the detailed structural and functional analyses using robust stereological techniques to quantify tubular length, glomerular and kidney volumes. Its limitation is first and foremost related to the fact that the study was conducted in experimental animals rather than in humans. While there have been a large number of clinical studies that have examined the renal effects of SGLT2 inhibition, these have, understandably, focused on kidney function rather than structure. The data herein complement another study that showed an increase in cell size of the S3 segment in response to another SGLT2 inhibitor, empagliflozin[33]. The present study adds to this by demonstrating that the S3 segment actually increases in length and that early transient cell proliferation is a key feature in its development.

Beyond the experimental animal context, we noted one SGLT2 inhibitor study in which CT imaging was used to measure kidney length at baseline and at study end[34]. In that study of 62 patients with type two diabetes and moderately good glycemic control (mean HbA1c 7.7%), Sugiyama *et al.* found that subjects who were treated with dapagliflozin displayed an increase in kidney length, as measured by CT, while those receiving non-SGLT2-based treatment experienced no change in kidney size, despite equivalent glucose reduction[35].

Finally, although the current study provides a cogent explanation for the less-than-predicted glucosuria with SGLT2 inhibition, we are cognizant of the fact that it was not conducted in humans and that other mechanisms such as post-translational modification of the transporter[36] that were not explored in the present study may also contribute.

ACKNOWLEDGMENTS

This study was supported by a grant from the Morris A. Hunter Charitable Trust and by an investigator-initiated grant from Astra Zeneca who had no influence on the study design, methodology, or interpretation. Dr. Gilbert is the Canada Research Chair in Diabetes Complications, and this work was supported in part by the Canada Research Chairs' Program. Dr. Connelly is supported by the Keenan Chair in Research Leadership, St. Michael's Hospital.

DISCLOSURES

REG reports receiving other research grants to his institution from AstraZeneca and Boehringer Ingelheim; serving on advisory panels for AstraZeneca, Boehringer Ingelheim, and Janssen; receiving CME speaker honoraria from AstraZeneca, Bayer, Boehringer Ingelheim, and Janssen, all unrelated to the current study. He also reports being a shareholder in Certa Therapeutics and Fibrocor Therapeutics. KAC reports receiving research grants to his institution from AstraZeneca and Boehringer Ingelheim; serving on advisory panels for AstraZeneca, Boehringer Ingelheim, and Janssen; receiving CME speaker honoraria from AstraZeneca, Bayer, Boehringer Ingelheim, and Janssen, all unrelated to the current study. KAC is supported by a Merit award from the Department of Medicine, University of Toronto, and the Keenan chair for Research Leadership at the Keenan Research Centre for Biomedical Science, Toronto.

Approval of the research protocol: N/A.
Informed consent: N/A.
Registry and the registration no. of the study/trial: N/A.
Animal studies: All animal studies were approved by the St. Michael's Hospital Animal Care Committee in accordance with the NIH's Guide for the Care and Use of Laboratory Animals, 8th Edition, 2011.

REFERENCES

1. Vallon V, Thomson SC. The tubular hypothesis of nephron filtration and diabetic kidney disease. *Nat Rev Nephrol* 2020; 16: 317–336.

2. Vallon V, Platt KA, Cunard R, *et al*. SGLT2 mediates glucose reabsorption in the early proximal tubule. *J Am Soc Nephrol* 2011; 22: 104–112.
3. Kriz W, Bankir L. A standard nomenclature for structures of the kidney. *Kidney Int* 1988; 33: 1–7.
4. Vrhovac I, Balen Eror D, Klessen D, *et al*. Localizations of Na(+)-D-glucose cotransporters SGLT1 and SGLT2 in human kidney and of SGLT1 in human small intestine, liver, lung, and heart. *Pflugers Arch* 2015; 467: 1881–1898.
5. Liu JJ, Lee T, DeFronzo RA. Why do SGLT2 inhibitors inhibit only 30–50% of renal glucose reabsorption in humans? *Diabetes* 2012; 61: 2199–2204.
6. Powell DR, DaCosta CM, Gay J, *et al*. Improved glycemic control in mice lacking Sglt1 and Sglt2. *Am J Physiol Endocrinol Metab* 2013; 304: E117–E130.
7. Rasch R, Norgaard JOR. Renal enlargement: comparative autoradiographic studies of ^{3}H-thymidine uptake in diabetic and uninephrectomised rats. *Diabetologia* 1983; 25: 280–287.
8. Rasch R, Dørup J. Quantitative morphology of the rat kidney during diabetes mellitus and insulin treatment. *Diabetologia* 1997; 40: 802–809.
9. Seyer-Hansen K, Hansen J, Gundersen HJG. Renal hypertrophy in experimental diabetes: a morphometric study. *Diabetologia* 1980; 18: 501–505.
10. Seyer-Hansen K. Renal hypertrophy in experimental diabetes. *Kidney Int* 1983; 23: 643–646.
11. Kriz W, Kaissling B. Structural organization of the mammailan kidney (Chapter 20). Seldin and Giebisch's the Kidney: Physiology & Pathophysiology, 4th edn. Amsterdam; Boston: Elsevier Inc., Academic Press, 2008.
12. Connelly KA, Wu E, Visram A, *et al*. The SGLT2i dapagliflozin reduces RV mass independent of changes in RV pressure induced by pulmonary artery banding. *Cardiovasc Drugs Ther* 2024; 38: 57–68.
13. Bellin AR, Zhang Y, Thai K, *et al*. Impaired SIRT1 activity leads to diminution in glomerular endowment without accelerating age-associated GFR decline. *Physiol Rep* 2019; 7: e14044.
14. Tanner GA, Vijayalakshmi K, Tanner JA. Effects of potassium citrate/citric acid intake in a mouse model of polycystic kidney disease. *Nephron* 2000; 84: 270–273.
15. Advani A, Kelly DJ, Advani SL, *et al*. Role of VEGF in maintaining renal structure and function under normotensive and hypertensive conditions. *Proc Natl Acad Sci USA* 2007; 104: 14448–14453.
16. Kelly DJ, Zhang Y, Moe G, *et al*. Aliskiren, a novel renin inhibitor, is renoprotective in a model of advanced diabetic nephropathy in rats. *Diabetologia* 2007; 50: 2398–2404.
17. Sadeghinezhad J, Nyengaard JR. Cat kidney glomeruli and tubules evaluated by design-based stereology. *Anat Rec (Hoboken)* 2019; 302: 1846–1854.
18. Nyengaard JR. Stereologic methods and their application to kidney research. *J Am Soc Nephrol* 1999; 10: 1100–1123.
19. Lane PH, Steffes MW, Mauer SM. Estimation of glomerular volume: a comparison of four methods. *Kidney Int* 1992; 41: 1085–1089.
20. Schindelin J, Arganda-Carreras I, Frise E, *et al*. Fiji: an open-source platform for biological-image analysis. *Nat Methods* 2012; 9: 676–682.
21. Rueden CT, Schindelin J, Hiner MC, *et al*. ImageJ2: ImageJ for the next generation of scientific image data. *BMC Bioinformatics* 2017; 18: 529.
22. Wassef L, Kelly DJ, Gilbert RE. Epidermal growth factor receptor inhibition attenuates early kidney enlargement in experimental diabetes. *Kidney Int* 2004; 66: 1805–1814.
23. Wang F, Flanagan J, Su N, *et al*. RNAscope: a novel in situ RNA analysis platform for formalin-fixed, paraffin-embedded tissues. *J Mol Diagn* 2012; 14: 22–29.
24. Zhang Y, Connelly KA, Thai K, *et al*. Sirtuin 1 activation reduces transforming growth factor-beta1-induced fibrogenesis and affords organ protection in a model of progressive, experimental kidney and associated cardiac disease. *Am J Pathol* 2017; 187: 80–90.
25. Vallon V. Molecular determinants of renal glucose reabsorption. Focus on "glucose transport by human renal Na+/D-glucose cotransporters SGLT1 and SGLT2". *Am J Physiol Cell Physiol* 2011; 300: C6–C8.
26. Vallon V, Rose M, Gerasimova M, *et al*. Knockout of Na-glucose transporter SGLT2 attenuates hyperglycemia and glomerular hyperfiltration but not kidney growth or injury in diabetes mellitus. *Am J Physiol Renal Physiol* 2013; 304: F156–F167.
27. Zerbini G, Bonfanti R, Meschi F, *et al*. Persistent renal hypertrophy and faster decline of glomerular filtration rate precede the development of microalbuminuria in type 1 diabetes. *Diabetes* 2006; 55: 2620–2625.
28. Rigalleau V, Garcia M, Lasseur C, *et al*. Large kidneys predict poor renal outcome in subjects with diabetes and chronic kidney disease. *BMC Nephrol* 2010; 11: 3.
29. Tuttle KR. Back to the future: glomerular hyperfiltration and the diabetic kidney. *Diabetes* 2017; 66: 14–16.
30. Denic A, Mathew J, Lerman LO, *et al*. Single-nephron glomerular filtration rate in healthy adults. *N Engl J Med* 2017; 376: 2349–2357.
31. Feldt-Rasmussen B, Mathiesen ER, Hegedus L, *et al*. Kidney function during 12 months of strict metabolic control in insulin-dependent diabetic patients with incipient nephropathy. *N Engl J Med* 1986; 314: 665–670.
32. Wiseman MJ, Saunders AJ, Keen H, *et al*. Effect of blood glucose control on increased glomerular filtration rate and kidney size in insulin-dependent diabetes. *N Engl J Med* 1985; 312: 617–621.
33. Sinha F, Federlein A, Biesold A, *et al*. Empagliflozin increases kidney weight due to increased cell size in the proximal tubule S3 segment and the collecting duct. *Front Pharmacol* 2023; 14: 1118358.

34. Cheong B, Muthupillai R, Rubin MF, *et al*. Normal values for renal length and volume as measured by magnetic resonance imaging. *Clin J Am Soc Nephrol* 2007; 2: 38–45.
35. Sugiyama S, Jinnouchi H, Kurinami N, *et al*. Impact of dapagliflozin therapy on renal protection and kidney morphology in patients with uncontrolled type 2 diabetes mellitus. *J Clin Med Res* 2018; 10: 466–477.
36. Arthur S, Coon S, Kekuda R, *et al*. Regulation of sodium glucose co-transporter SGLT1 through altered glycosylation in the intestinal epithelial cells. *Biochim Biophys Acta* 2014; 1838: 1208–1214.